

Electronic Supplementary Information (ESI) for

**A nanofluidic osmotic power generator demonstrated in polymer gel electrolytes with
substantially enhanced performance**

Li-Hsien Yeh,^{1,*} Zih-Ying Huang,^{1,2} Yi Cheng Liu,³ Ming-Jay Deng,^{4,5} Tzung-Han Chou,²

Hsing-Chiao Ou Yang,¹ Tansir Ahamad,⁶ Saad M. Alshehri,⁶ Kevin C. W. Wu³

¹Department of Chemical Engineering, National Taiwan University of Science and
Technology, Taipei 10607, Taiwan

²Department of Chemical and Materials Engineering, National Yunlin University of Science
and Technology, Yunlin 64002, Taiwan

³Department of Chemical Engineering, National Taiwan University, Taipei 10617, Taiwan

⁴Bachelor Program in Interdisciplinary Studies, National Yunlin University of Science and
Technology, Yunlin 64002, Taiwan

⁵Department of Applied Chemistry, Providence University, Taichung 43301, Taiwan

⁶Department of Chemistry, College of Science, King Saud University, P.O. Box 2455,
Riyadh 11451, Saudi Arabia

* Corresponding Author: lhyeh@mail.ntust.edu.tw, Tel. +886-2-27376942

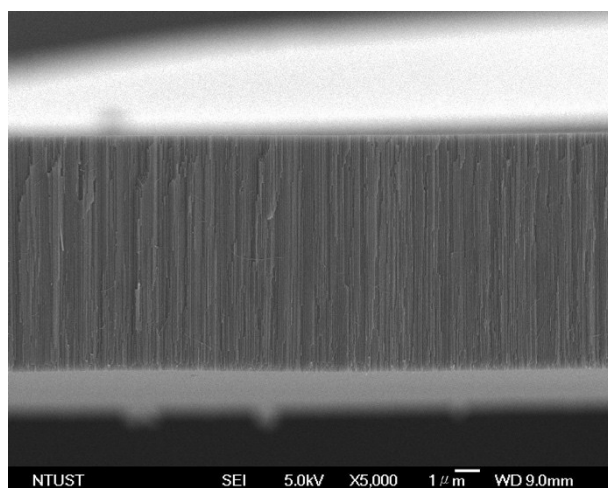


Figure S1. Cross-section view SEM image of the prepared ANM, revealing highly ordered structure of straight channels.

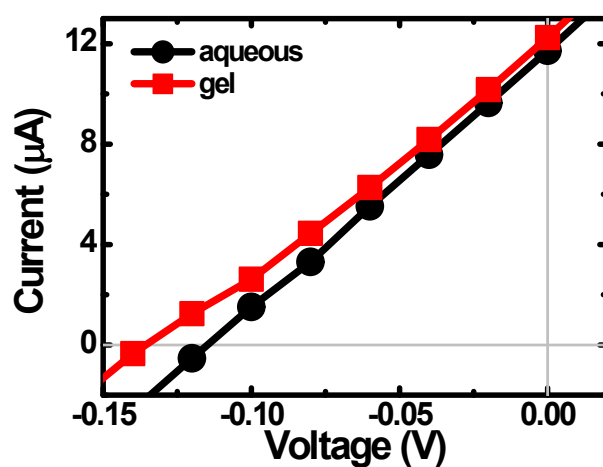


Figure S2. I-V curves of the ANM in aqueous and PVA gel electrolytes under 500 mM/0.1 mM KCl gradient.

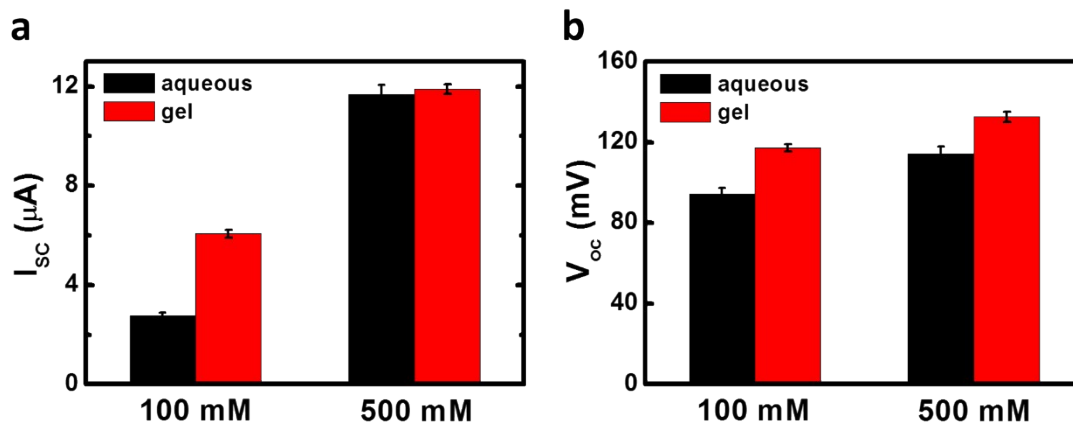


Figure S3. (a) Short-circuit current I_{sc} and (b) open-circuit voltage V_{oc} generated by the ANM placed in contact with aqueous and PVA gel electrolytes as a function of KCl gradient. A lower concentration of KCl was kept at 0.1 mM as reported in Fig. 2a of the main text.

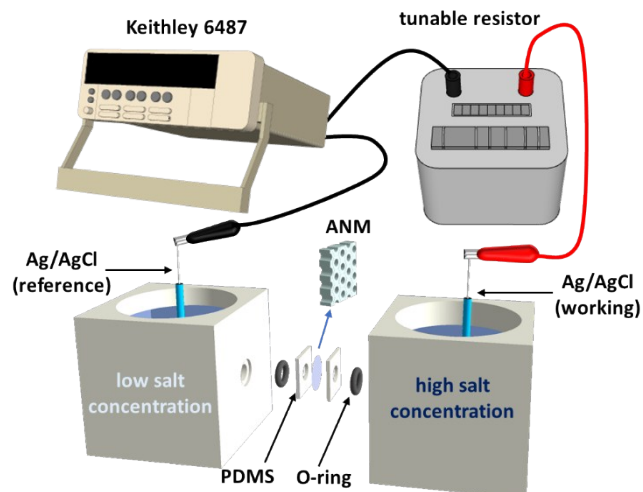


Figure S4. Schematic illustration of the experimental set-up for the osmotic power generation.

The power generated can be transferred to the external circuit containing a tunable resistor.

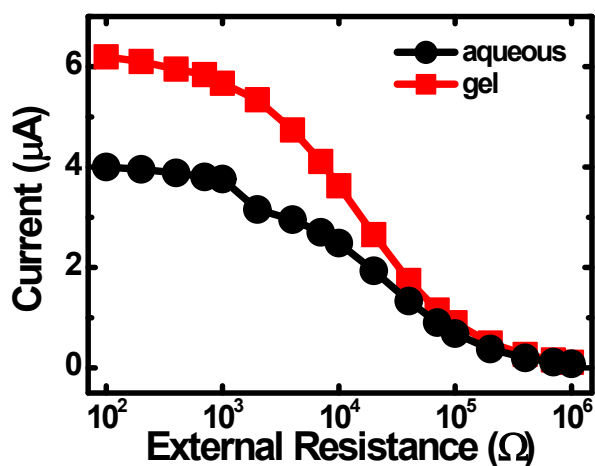


Figure S5. Comparison of the current generation in aqueous solution with that in PVA gel solution in a 100 mM/0.1 mM KCl gradient. This is the same ANM as shown in Fig. 2 of the main text.

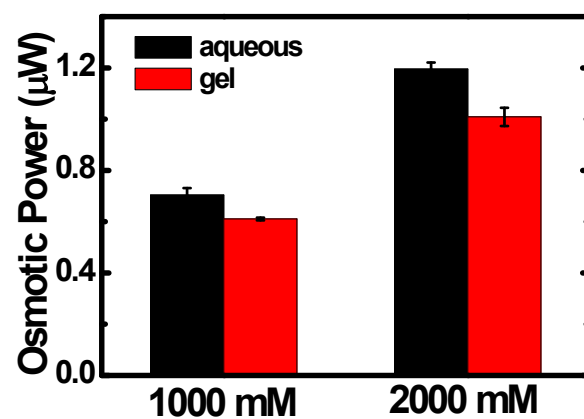


Figure S6. Osmotic power generation in aqueous and PVA gel electrolytes as a function of KCl gradient. Here a lower concentration of KCl was kept at 0.1 mM as reported in Fig. 2c of the main text.

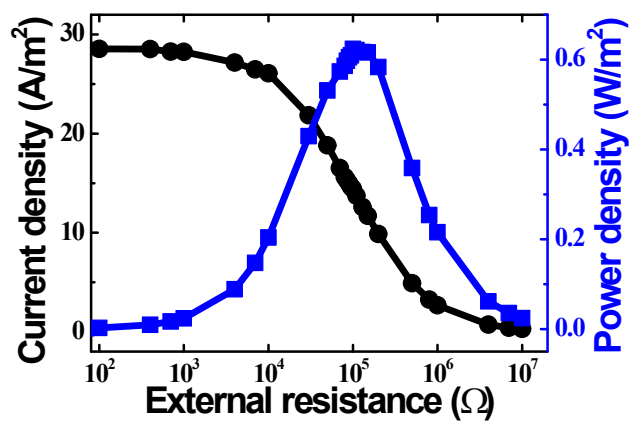


Figure S7. Osmotic current density and power density generated in the PVA gel subjected to a 100 mM/0.1 mM KCl gradient. The maximum power density generated is ~ 0.624 W/m². The result was extracted from another independently prepared ANM.

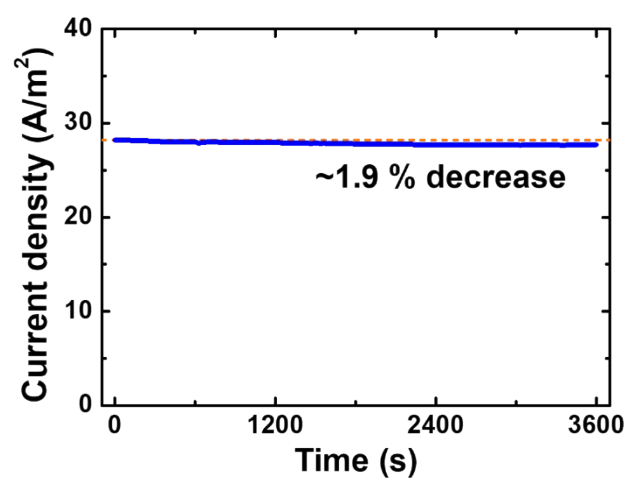


Figure S8. Current density-time curve of the PVA-gel electrolyte system in a 100 mM/0.1 mM

KCl gradient, exhibiting ~1.9 % decrease in an hour for the case of no electrolyte replenishing.

Numerical Simulation

In the model, we considered the two nanochannel systems (Fig. 4), connected by two large, identical reservoirs. The energy harvesting from a salinity gradient for the systems considered in the main text can be described by the modified Poisson and Nernst-Planck equations:¹

$$-\nabla^2 \phi = \frac{\sum_{i=1}^2 F z_i C_i + \Phi \rho_{PE}}{\epsilon_f}, \quad (\text{S1})$$

$$\nabla \cdot \mathbf{J}_i = \nabla \cdot \left[-D_i \nabla C_i - \left(\frac{F z_i C_i D_i}{RT} \right) \nabla \phi \right] = 0, \quad (\text{S2})$$

In the above, ϕ is the electric potential; ϵ_f is the fluid permittivity; F , R , and T are the Faraday constant, gas constant, and absolute temperature, respectively. C_i , D_i , \mathbf{J}_i , and z_i are the concentration, diffusivity, flux, and valence of the i^{th} ionic species, respectively ($i = 1$ for K^+ cations and $i = 2$ for Cl^-). The charged PVA in the channel is modeled as a polyelectrolyte (PE) layer, which is ion-penetrable and homogeneously structured with a fixed space charge density of ρ_{PE} . In the model of the solid-nanochannel system (Fig. 4a in the main text), we let $\Phi = 0$. Otherwise, in the model of the PE-filled nanochannel (Fig. 4b), we let $\Phi = 1$ ($\Phi = 0$) for the region inside (outside) the PE layer. The radial-axial domain (r, z) is considered to simulate the cylinder-shaped structure of the ANM used. The detailed boundary conditions required can be found in our previous publications.^{1, 2}

The current-voltage curves for the systems considered in Fig. 4 are solved numerically based on the above-mentioned model performed by COMSOL Multiphysics 4.3a operated on a high-

performance cluster. The ionic current through the channel can be calculated by

$$\int_S \left(\sum_{i=1}^2 Fz_i \mathbf{J}_i \right) \cdot \mathbf{n} dS, \quad (\text{S3})$$

where \mathbf{n} is unit normal vector and S denotes either end of two reservoirs.

References

1. C. Y. Lin, C. Combs, Y. S. Su, L. H. Yeh and Z. S. Siwy, *J. Am. Chem. Soc.*, 2019, **141**, 3691-3698.
2. L. H. Yeh, M. Zhang, N. Hu, S. W. Joo, S. Qian and J. P. Hsu, *Nanoscale*, 2012, **4**, 5169-5177.